Chapter 8
Fracture Response of Cross-Linked Epoxy Resins at High Loading Rate as a Function of Glass Transition Temperature

John A. O'Neill, C. Allan Gunnarsson, Paul Moy, Kevin A. Masser, Joseph L. Lenhart, and Tusit Weerasooriya

Abstract The failure behavior of cross-linked polymer epoxies with different glass transition temperatures (Tg) was investigated under Mode I fracture at high loading rate using a novel experimental method with in situ observation of the fracture process. By varying the monomer choices, the properties of the epoxies can be tailored to achieve greater resistance to cracking and higher impact toughness. For these experiments, a unique four-point bending specimen was used. High rate experiments were conducted on a modified split Hopkinson pressure bar with pulse-shaping. High speed digital imaging was used to visualize failure initiation. The images were also used with digital image correlation to optically measure the crack opening displacement and crack propagation velocity. The experimental results were used to calculate the energy required to initiate fracture at high loading rate. The results indicate that the critical energy required to initiate fracture at high loading rate was higher for epoxies with lower Tg values, up to an optimum Tg. This dependence of critical energy on the Tg of the epoxy was similar to that which has been previously measured for the epoxy's impact resistance. In this paper, the experimental methods and results are discussed.

Keywords High Strain Rate • Glass Transition Temperature • Epoxy • Fracture Response • Mode I Fracture • Hopkinson Bar

8.1 Introduction

Polymer epoxies are frequently used in many applications to structurally bond components of similar or dissimilar materials. Some of the many uses can be found in the form of fiber reinforced polymers (FRP) for the aerospace and automotive industries, sporting goods, and marine crafts. When exposed to sudden impacts, these structural components and bonds are subjected to high loading rates. Typically, the failure of the resin matrix in FRPs is the dominating factor leading to interply delamination. Therefore, it is important to understand how these epoxies behave and fail at high loading rate. High loading rates are especially important as they are characteristic of blast and ballistic impact.

The fracture response of polymer epoxies has been investigated by many researchers. At quasi-static loading rates, studies have been performed to understand crack initiation, the effects of molecular weight between cross-links, and the fracture behavior of epoxy systems using various toughners. Specimen geometries based on various ASTM standards have been developed for both three and four point bend specimen geometries [1–6].

Experimental techniques for dynamic fracture behavior have been developed and can be summarized into three categories: high rate bending, high rate tension, and dynamic wedging. Many different techniques exist; some of these have been summarized previously by Jiang et al. [7]. Previous studies have shown that there are two important criteria for valid and useful high rate fracture experiments: a state of dynamic equilibrium of the specimen, and a constant loading rate of the specimen during the experiment. Both of these criteria can be obtained by shaping the input loading pulse [8–14]. Additionally, low impedance materials, such as pre-cracked beams and polymer materials, frequently cause traditional strain gauge measurement techniques to be unusable. Other researchers, such as Chen et al. [9], have solved this problem by embedding quartz based loading devices in the loading train, which allows for direct measurement of dynamic equilibrium and loading rate. Weerasooriya et al. developed an experimental method to measure fracture toughness under four-point

Certain commercial equipment, instruments, or materials are identified in this paper in order to specify the experimental procedure adequately. Such identification is not intended to imply recommendation or endorsement by the Army Research Laboratory, nor is it intended to imply that the materials or equipment identified are necessarily the best available for the purpose.

J.A. O'Neill • C.A. Gunnarsson • P. Moy • K.A. Masser • J.L. Lenhart • T. Weerasooriya (✉)
Army Research Laboratory, Aberdeen Proving Ground, Aberdeen, MD 21005, USA
e-mail: tusit.weerasooriya.civ@mail.mil

D. Casem et al. (eds.), *Dynamic Behavior of Materials, Volume 1*, Conference Proceedings of the Society for Experimental Mechanics Series, DOI 10.1007/978-3-319-41132-3_8

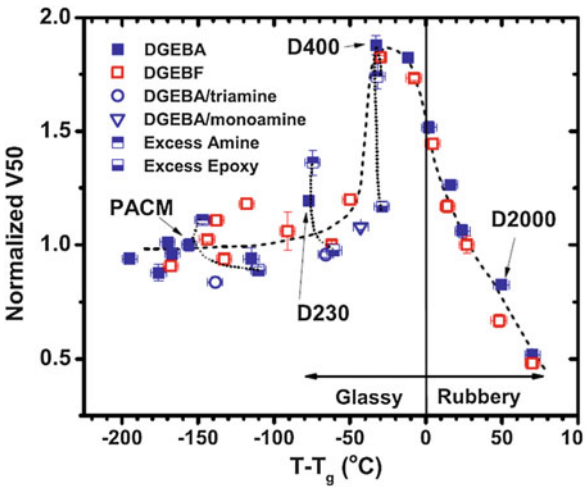

Fig. 8.1 Normalized impact resistance (V50) data for a series of epoxy networks as a function of reduced temperature [1]

bend at high loading rates, and used it to measure the dynamic fracture toughness of SiCN ceramic [10] and PMMA [11]. Gunnarsson et al. [12] further developed this technique to measure the fracture toughness of human cortical bone, integrating ultra-high speed imaging and crack tip strain analysis. Syn et al. [13] studied the surface morphology effect on the fracture behavior along dissimilar material interfaces (in this case, aluminum and epoxy) using a wing-like specimen. Weerasooriya et al. [14] used a similar method to study the dynamic failure behavior of adhesive bond interfaces. Both Weerasooriya et al. and Syn et al. showed an increase in failure load and energy rate for fracture initiation as loading rate increased from low to high rates.

Previous investigations have demonstrated that the proximity of the testing temperature to the glass transition temperature strongly influences the ballistic performance of amine-cured epoxy networks [15, 16]. Epoxy/amine mixtures well into the glassy state (DGEBA/PACM) or well into the rubbery state (DGEBA/D2000) perform relatively poorly, failing in a brittle manner in the case of DGEBA/PACM, or by complete projectile penetration of the rubbery material in the case of DGEBA/D2000. This is shown more clearly in Fig. 8.1. Epoxy/amine mixtures such as DGEBA/D400, whose glass transition temperature is close to the ballistic measurement temperature, fail through a combination of modes, exhibiting plastic deformation and radial and cone cracking. The observation that being close to the glass transition improves ballistic performance has also been observed by other researchers [17–20], and is likely a general trend of polymer networks.

In this investigation, the high rate fracture behavior of three amine-cured epoxy networks is characterized by conducting Mode I fracture experiments on epoxy (DGEBA-based) specimens with varying Tg. Epoxy (DGEBA) and amine mixtures were chosen such that they were well below (DGEBA/PACM), below (DGEBA/D230), or near (DGEBA/D400) the glass transition temperature, corresponding to a range of poor to relatively good ballistic performance. A fracture specimen was used similar to previous work [13, 14]. The specimen's loading surfaces, the nose and the two wing-tips, were designed to be curved instead of flat. This modification stiffened the loading nose of the specimen to reduce the potential of the specimen bending when loaded. It is important that the specimens do not bend, and that all energy absorbed is used to initiate failure and crack propagation. The effectiveness of the curved surface design in eliminating the bending problem in the specimens was verified using ultra high speed digital image correlation (DIC). An additional benefit is the ability to use flat-faced loading fixtures instead of pin-based loading fixtures. This allows for use of the incident and transmission bar ends to load the specimen, instead of special fixtures. Directly using the bar ends for specimen loading reduces experimental complexity, and improves wave transmission by removing changes in impedance in the loading train. All experiments were conducted at dynamic loading rate using an aluminum split pressure Hopkinson bar (SHPB) system. High sensitivity semi-conductor strain gages were used to accurately measure the bar strain histories and stresses at the loading interfaces to verify dynamic equilibrium. The experimental results were used to quantify the Tg dependence of DGEBA based polymer system fracture properties, such as crack propagation velocity (CPV), failure load, and failure energy. This research will provide a quantitative fracture-resistance experimental technique for evaluation of epoxy systems as a function of Tg. Future work will be performed to relate the failure load to the initiation fracture toughness.

8.2 Experimental

8.2.1 Materials

Diglycidyl ether of bisphenol A (DGEBA), i.e., EPON 825 (average molecular weight ~355 g/mol), was obtained from Miller-Stephenson [7] and was used as the epoxy. Three curing agents were used with the DGEBA: polypropylene oxide based-Jeffamine diamines with a vendor-specified molecular weight of 230 g/mol (D230) and 400 g/mol (D400) were provided by Huntsman. Diamine curing agent, 4,4'-methylenebis(cyclohexylamine) (PACM), was provided by Air Products. PACM is an unmodified cycloaliphatic amine commonly used in filament winding and wet layup laminating for fabrication of fiber-reinforced polymers, where high fracture toughness and better corrosive properties are necessary. All epoxies and curing agents were used as received without further purification. All formulations were stoichiometric mixtures of the epoxy and diamine curing agent. Sample designations are based on the amine curing agent used, e.g. D230 refers to a stoichiometric mixture of DGEBA and D230. The chemical structure of the epoxy and curing agents used in this study are shown in Fig. 8.2.

The high rate fracture specimen geometry is shown in Fig. 8.3 (all dimensions mm). Silicone molds were prepared by casting Dow Xiameter brand silicone RTV onto approximately 50 steel sample blanks. After curing, the sample blanks were removed, revealing high fidelity cavities. The molds were coated with several layers of mold release to aide sample removal. For all sample preparations, epoxies and curing agents were preheated to 60 °C. Each epoxy and diamine was then mixed and stirred vigorously at 60°C for 5 min, poured into silicone molds, and degassed under vacuum. Every epoxy mixture appeared uniformly mixed, with no phase separation visible. All epoxies were cured under a nitrogen purge with a cure cycle of 80°C for 2 h, 150°C for 8 h, and 200°C for 2 h. This cure cycle has been shown to result in networks where no uncured functional groups can be detected.

The complexity of the fracture geometry prevented the use of an aluminum mold to direct cast the epoxy into the fracture geometry. This is due to the difficultly in extracting the epoxy from an aluminum mold without damaging the sample even if

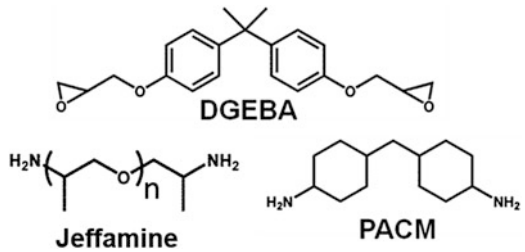

Fig. 8.2 Chemical structures of DGEBA, the general structure of the Jeffamine series (D230, D400) and the chemical structure of the PACM diamine

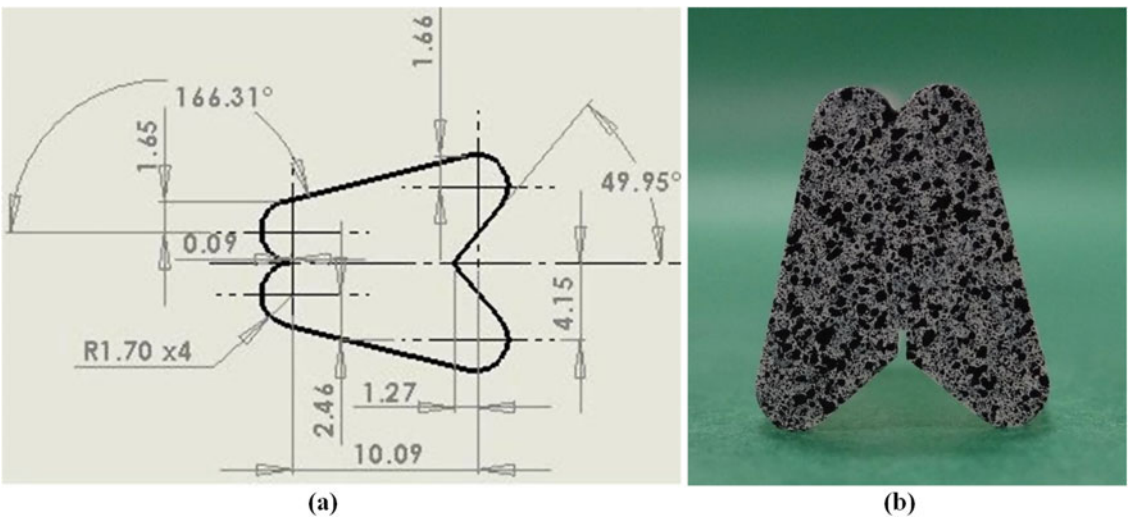

Fig. 8.3 (**a**) Fracture specimen geometry and (**b**) typical specimen with notch and DIC speckle pattern

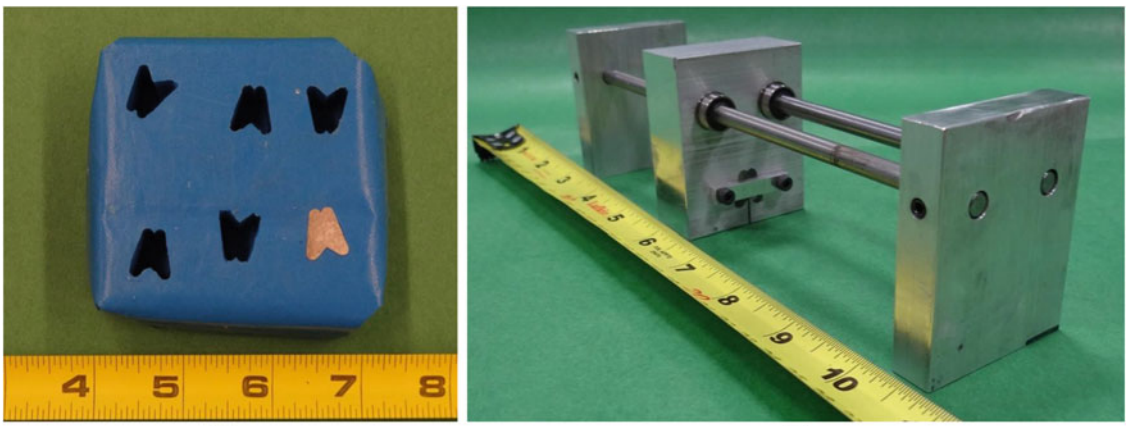

Fig. 8.4 (**a**) Silicon mold used to mold the epoxy and (**b**) custom notching fixture

mold release is applied. Instead, a flexible silicon mold was created. To fabricate the mold, fracture specimens with the geometry as shown in Fig. 8.3 were machined from 25.4 mm thick aluminum and cast in silicon. The flexibility of the silicone enabled the replicate aluminum specimens to be removed from the silicone mold once the mold was cured. An example of the silicone mold is shown in Fig. 8.4. The epoxy mixture could then be poured into the silicon mold and cured.

Once the epoxy specimens were finished curing, they were pressed out of the mold and milled to a thickness of 23.25 mm using a table mill. This process was necessary to remove the uneven material present near the mold surfaces after curing and to create flat and parallel surfaces. With the specimens at the proper length, a notch was cut with a 300 μm width diamond saw blade. The present study did not investigate any other pre-crack profile other than the notch created from the saw blade. A custom fixture (Fig. 8.4b) for specimen notching was designed to create a constant 1 mm deep notch into the center of each specimen as shown in Fig. 8.3b.

8.2.2 High Rate Fracture Experiments

Dynamic epoxy fracture experiments were conducted on a modified SHPB. The working principle of this experimental setup is well documented [7–10, 21]. The bars used for the incident and transmission bar in the test setup were made from Al 7075 with a diameter of 31.8 mm and a length of 3.66 m. A gas gun propelled Al 7075 striker with a length of 0.61 m was used to generate a stress pulse in the incident bar. Pulse shaping was used to shape the input pulse to achieve the necessary dynamic equilibrium and a near constant loading rate. Semi-conductor strain gages were mounted at the midpoints of the input and output bars to record the bar stress histories. Semi-conductor gages were used for their high sensitivity, allowing for measurement of the low amplitude pulse in the transmission bar and the slight difference between incident and reflected pulse in the incident bar. Semi-conductor strain gages are much more sensitive to ambient temperature and humidity than traditional strain gages; therefore a calibration for the semi-conductor strain gages was conducted before each test series, using a known compressive strain pulse measured using standard resistive strain gages. The dynamic experiments had a relative bar velocity of about 5.0 m/s, which corresponded to a loading rate of approximately 100 MN/s. To capture the onset of crack initiation and propagation, an ultra-high-speed camera was used to record at a frame rate of 250 K fps. The specimen was oriented in the SHPB so that the pre-crack side was at the incident bar interface, as shown in Fig. 8.5.

DIC was used to accurately measure the displacement of the specimen's two wings relative to each other. DIC is an optical method which uses sequential images to measure full-field displacement and deformation of an object under load. To summarize the DIC process, a speckled pattern is applied on the surface of the specimen and sequential images are captured using a digital camera throughout an experiment. The digital images are then post-processed to compute the deformation and displacement field by tracking the movement of the speckles. In this study, the relative displacement was extracted between two selected points, one on each of the specimen's wings. These displacement measurements corresponded to digital extensometers measuring the perpendicular distances across the crack, and were used to obtain the crack opening displacement (COD) as a function of time during the experiment. COD is the distance that the two halves of the specimen separate away from each other as the crack progagates along the specimen length.

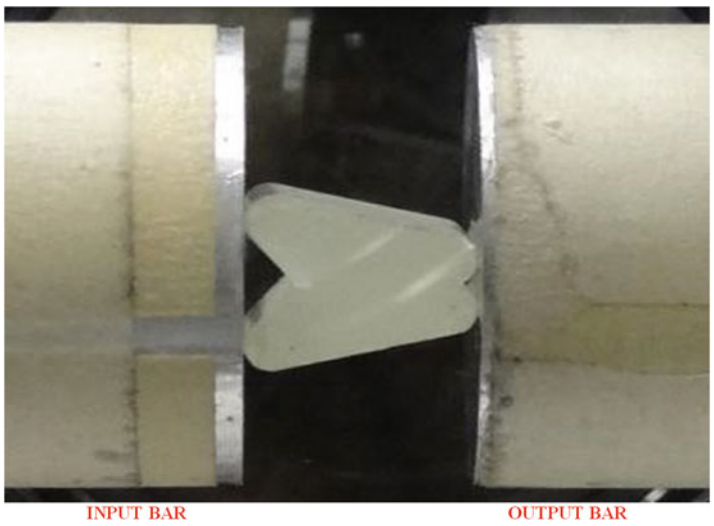

Fig. 8.5 Mode I epoxy fracture specimen loaded in SHPB (speckle surface faces away, towards camera)

8.3 Results and Discussion

8.3.1 Crack Propagation Velocity

DIC was used to calculate the COD at various locations along the specimen using digital extensometers, similar to bonded crack detection gages. These extensometers and their locations are shown in Fig. 8.6a. The COD at each of these locations was extracted and plotted together (Fig. 8.6b). By visually inspecting the images for crack tip arrival at an extensometer location, and comparing this to the corresponding extensometer's COD, it was determined that the crack had reached the extensometer location when the COD reached 0.5 pixels. The time at which each extensometer reached 0.5 pixel was extracted, and compared to the location of the extensometer along the specimen length to extract a time-crack tip location relationship.

The digital extensometer results indicated that the crack traveled at a linear rate (constant velocity) along the specimen. As an example, Fig. 8.7 shows the crack location as a function of time for a single PACM specimen under a high loading rate experiment. The five data points correspond to the five digital extensometers used for this experiment; the time value of each data point is the amount of time it required for each extensometer to measure a length increase (COD) of 0.5 pixels. The crack tip location followed a linear trend and the slope of the linear fit to the points indicates the crack tip propagation velocity (CPV), in this case 234.4 m/s.

8.3.2 Failure Load and Energy

The failure load is simply the maximum force that the specimen experienced during the experiment. Future work will relate this failure load to the fracture toughness (K_I) of the material. The failure energy is the energy required to initiate crack propagation from the original precrack tip. Failure energy was calculated using Eq. 8.1 by integrating load history with respect to displacement, from zero displacement to the displacement corresponding to crack growth.

$$FE = \int_{x_o}^{x_{crack\ \ growth}} P(x)\, dx \tag{8.1}$$

Table 8.1 shows a summary of the average results of the Mode I fracture DGEBA epoxy experiments at the dynamic loading rate, including plus/minus statistics representing plus/minus one standard deviation of the data. Figure 8.8 shows these results graphically as a function of the reduced temperature for (a) crack propagation velocity, (b) crack initiation load, and (c) failure energy. The reduced temperature (T−Tg) is simply the material Tg subtracted from the material temperature at time of testing (here, for all experiments, room temperature, or 23 °C). In each plot, the black dots represent the average value for each loading rate. The results show that all three fracture parameters for DGEBA epoxy increased when the Tg

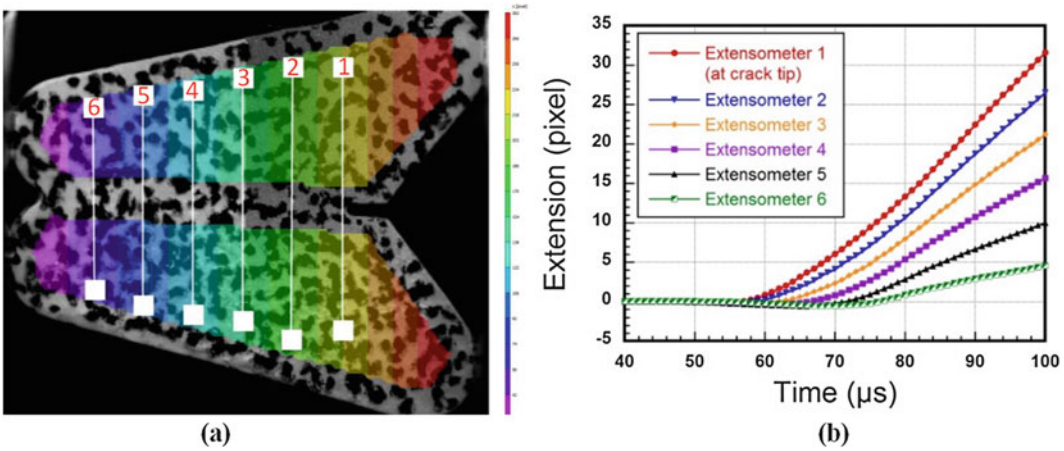

Fig. 8.6 (**a**) Location of digital extensometers across specimen and (**b**) COD of extensometers vs time

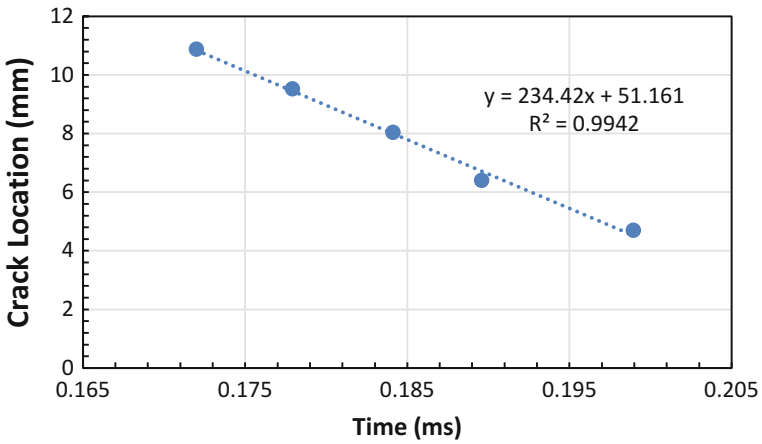

Fig. 8.7 Example of crack location vs time for a PACM specimen under high-rate loading

Table 8.1 Summary of results for Mode I fracture experiments of DGEBA-based epoxies at high-loading rate

Cure agent	Tg (°C)	T−Tg (°C)	Crack propagation velocity (m/s)	Failure load (kN)	Failure energy (J)
PACM	160	−137	234.47 ± 16.65	9.101 ± 0.596	1.502 ± 0.357
D230	90	−67	302.79 ± 47.62	10.916 ± 1.224	2.373 ± 0.786
D400	45	−22	291.96 ± 43.43	10.485 ± 1.788	2.989 ± 1.409

decreased from 160 to 90 °C, corresponding to a change in cure agent from PACM to D230. However, both CPV and failure load decreased slightly when the Tg decreased from 90 to 45 °C, with the cure agent changed from D230 to D400,. The failure energy showed a clear trend, linearly increasing as the T−Tg increased (Tg decreased). The failure energy was greatest for the DGEBA formulation that utilized D400 as the cure agent, which represents a Tg for the epoxy that is closest to the apparent ideal Tg for impact protection.

8.4 Conclusions

Mode I fracture experiments were conducted at high loading rate on DGEBA epoxy based systems using a unique fracture specimen geometry. The Tg of the epoxy system was varied by altering the curing agent, so that the fracture properties of the DGEBA epoxy could be studied as a function of Tg. High speed imaging was utilized to accurately deterimine the timing of crack initiation/failure, and DIC was used to measure the crack propagation velocity. The results show that the measured

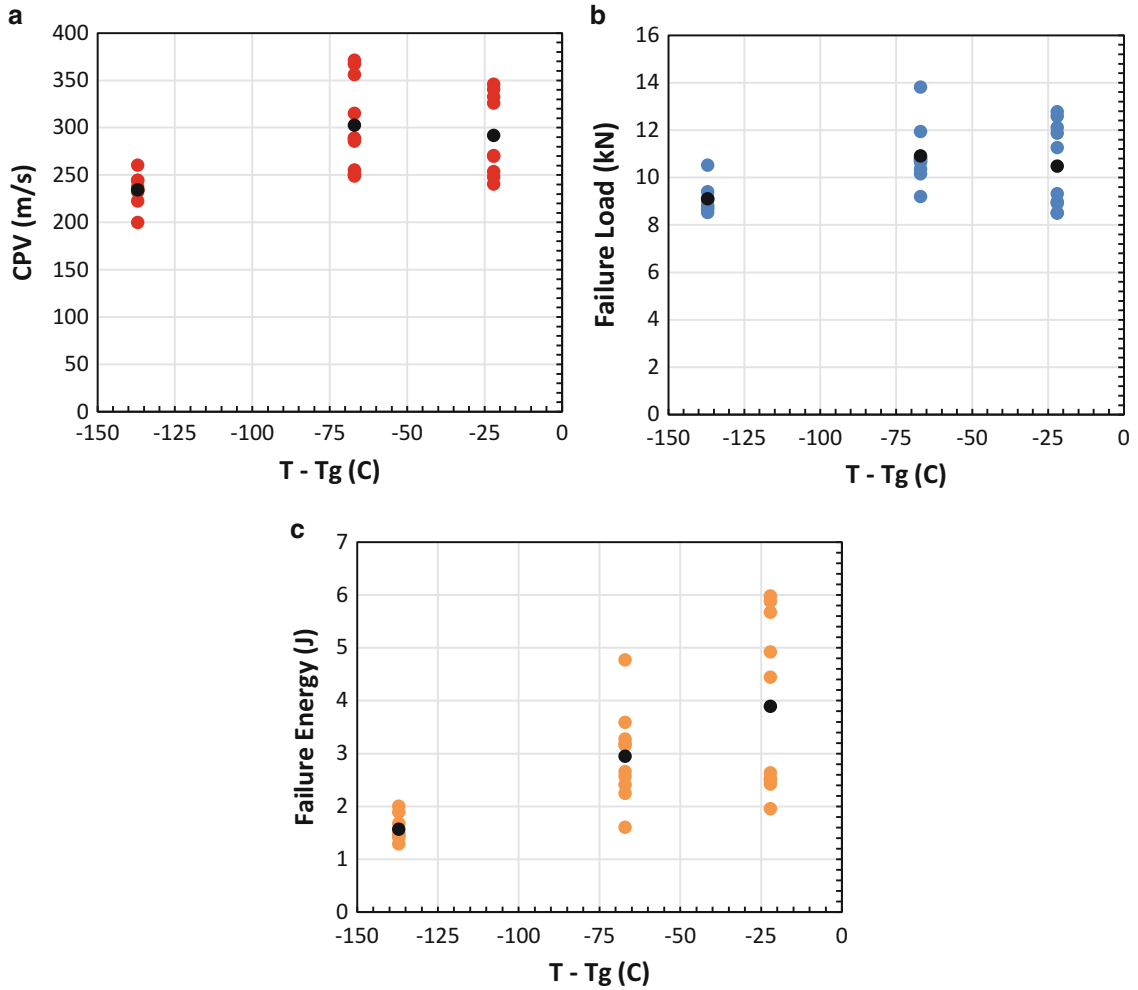

Fig. 8.8 Relationship between the curing agent glass transition temperature and (**a**) crack propagation velocity, (**b**) failure load, and (**c**) failure energy

critical fracture parameters for DGEBA epoxy increase when the cure agent was altered from PACM to D230 (Tg decreased from 160 to 90 °C). However, both CPV and failure load decreased slightly as the cure agent was again changed from D230 to D400, with the Tg decreasing from 90 to 45 °C. On the other hand, there was a clear linear trend of increasing failure energy as the reduced temperature (T−Tg) increased, corresponding to decreasing epoxy Tg. The failure energy was greatest for the D400-DGEBA formulation, which represents a reduced temperature (T−Tg) closest to the point which has demonstrated maximum impact resistance. Future studies will investigate the effect of moving the cure agent Tg to the rubbery region, other epoxy systems with dispersed toughenners, changing the cross-link density, and molecular weight. Additionally, the rate dependence of the fracture properties shown here will be investigated for lower loading rates.

References

1. Cho, K., Lee, D., Park, C.E., Huh, W.: Effect of molecular weight between crosslinks on fracture behaviour of diallylterephthalate resins. Polymer **37**(5), 813–817 (1996)
2. Kang, B.U., Jho, J.Y., Kim, J., Lee, S., Park, M., Lim, S.: Effect of molecular weight between crosslinks on the fracture behavior of rubber-toughened epoxy adhesives. J. Appl. Polym. Sci. **79**, 38–48 (2001)
3. Hussain, M., Nakahira, A., Nishijima, S., Niihara, K.: Fracture behavior and fracture toughness of particulate filled epoxy composites. Mater. Lett. **27**, 21–25 (1996)
4. Mostovoy, S., Ripling, E.J.: Fracture toughness of an epoxy system. J. Appl. Polym. Sci. **10**, 1351–1371 (1966)

5. Wakako, A., Kentaro, N., Tadaharu, A., Akihiko, Y.: Fracture toughness for mixed mode I/II of epoxy resin. Acta Mater. **53**(3), 869–875 (2005)
6. Cho, K., Huh, W.: Effect of molecular weight between crosslinks on fracture behaviour of diallylterephthalate resins. Polymer **37**(5), 813–817 (1996)
7. Jiang, F., Vecchio, K.: Hopkinson Bar loaded fracture experimental technique: A critical review of dynamic fracture toughness tests. Appl. Mech. Rev. **62** (2009). Transactions of the ASME
8. Wu, X.J., Gorham, D.A.: Stress equilibrium in the split Hopkinson pressure Bar test. J. Phys. IV **7**(C3), 91–96 (1997)
9. Chen, W., Lu, F., Zhou, B.: A quartz crystal imbedded split Hopkinson bar for soft materials. Exp. Mech. **40**(1), 1–6 (2000)
10. Weerasooriya, T., Moy, P., Casem, D., Cheng, M., Chen, W.: A four point bending load technique for determination of dynamic fracture toughness for ceramics. J. Am. Ceram. Soc. **89**(3), 990–995 (2006)
11. Weerasooriya, T., Moy, P., Casem, D., Cheng, M., Chen, W.: Fracture toughness for PMMA as a function of loading rate. Proceedings of the 2006 Society of Experimental Mechanics Annual Conference
12. Gunnarsson, C.A., Sanborn, B., Foster, M., Moy, P., Weerasooriya, T.: Initiation fracture toughness for human cortical bone as a function of loading rate. Proceedings of the 2012 Society of Experimental Mechanics Annual Conference
13. Syn, C., Chen, W.: Surface morphology effects on high-rate fracture of an aluminum epoxy interface. J. Compos. Mater. **42**, 1639–1658 (2008)
14. Weerasooriya, T., Gunnarsson, C.A., Jensen, R., Chen, W.: Strength and failure energy for adhesive interfaces as a function of loading rate. Proceedings of the 2011 Society of Experimental Mechanics Annual Conference
15. Knorr Jr., D.B., Yu, J.H., Richardson, A.D., Hindenlang, M.D., McAninch, I.M., La Scala, J.J., Lenhart, J.L.: Polymer **53**(25), 5917–5923 (2012)
16. Masser, K.A., Knorr Jr., D.B., Hindenlang, M.D., Yu, J.H., Richardson, A.D., Strawhecker, K.E., Beyer, F.L., Lenhart, J.L.: Polymer **58**, 96–106 (2015)
17. Bogoslovov, R.B., Roland, C.M., Gamache, R.M.: Impact-induced glass transition in elastomeric coatings. Appl. Phys. Lett. **90**, 221910 (2007)
18. Roland, C.M.: Rubber Chem. Technol. **79**(3), 429–459 (2006)
19. Roland, C.M., Fragiadakis, D., Gamache, R.M.: Compos. Struct. **92**(5), 1059–1064 (2010)
20. Roland, C.M., Fragiadakis, D., Gamache, R.M., Casalini, R.: Philos. Mag. **93**(5), 468–477 (2013)
21. Davies, E.D.H., Hunter, S.C.: The dynamic compression testing of solids by the method of the split Hopkinson pressure bar. J. Mech. Phys. Solids **11**(3), 155–179 (1963)